An Integration of Optimal Topology and Shape Design for Magnetostatics *

Dalibor Lukáš

SFB F013 "Numerical and Symbolic Scientific Computing", University Linz, Altenberger Strasse 69, A-4040 Linz, Austria
dalibor.lukas@vsb.cz, http://lukas.am.vsb.cz

Summary. Topology optimization searches for an optimal distribution of material and void without any restrictions on the structure of the design geometry. Shape optimization tunes the shape of the geometry, while the topology is fixed. In this paper we proceed sequentially with the optimal topology and shape design so that a coarsely optimized topology is the initial guess for the following shape optimization. In between we identify the topology by hand and approximate it by piecewise Bézier shapes by means of the least square method. For the topology optimization we use the steepest descent method, while a quasi–Newton method and multilevel techniques are used for the shape optimization. We apply the machinery to optimal design of a direct electric current electromagnet. The resulting optimal design corresponds to physical experiments.

1 Introduction

In the process of development of industrial components one looks for the parameters to be optimal subject to a proper criterion. The geometry is usually crucial as far as the design of electromagnetic components is concerned. We can employ topology optimization, cf. [Ben95], to find an optimal distribution of the material without any preliminary knowledge. Shape optimization, cf. [HN97, Luk04], is used to tune shapes of a known initial design. While in the structural mechanics topology optimization results in rather complicated structures the shapes of which are not needed to be then optimized, in magnetostatics we end up with simple topologies which, however, serve as very good initial points for the further shape optimization. The idea here is to couple them sequentially.

In [Cea00] a connection between topological and shape gradient is shown and applied in structural mechanics. They proceed shape and topology optimization simultaneously so that at one optimization step both the shape and

*This research has been supported by the Austrian Science Fund FWF within the SFB "Numerical and Symbolic Scientific Computing" under the grant SFB F013, subproject F1309.

topology gradient are calculated. Then shapes are displaced and the elements with great values of the topology gradient are removed, while introducing the natural boundary condition along the new parts, e.g. a hole. Here we are rather motivated by the approach in [OBR91, TCh01], where they apply a similar algorithm as we do to structural mechanics, however, using re-meshing in a CAD software environment, which was computationally very expensive. Our aim here is to make the algorithm fast. Therefore, we additionally employ semianalytical sensitivity analysis and a multilevel method.

2 Topology Optimization for Magnetostatics

Let us consider a fixed computational domain $\Omega \subset \mathbf{R}^d$, where $d = 2, 3$. Let $\Omega_\mathrm{d} \subset \Omega$ be the subdomain where the designed structure can arise. The set of admissible material distributions is denoted by $\mathcal{Q} := \{\rho \in L^2(\Omega_\mathrm{d}) \mid 0 \le \rho \le 1\}$. We penalize the intermediate values by

$$\widetilde{\rho}_p(\rho) := \frac{1}{2}\left(1 + \frac{1}{\arctan(p)}\arctan(p(2\rho - 1))\right),$$

where $p := 100$ is typically good enough. Further, we consider the following linear magnetic reluctivity:

$$\nu(\widetilde{\rho}) := \begin{cases} \nu_0 + (\nu_1 - \nu_0)\widetilde{\rho}, & \text{in } \Omega_\mathrm{d} \\ \nu_0, & \text{otherwise} \end{cases},$$

where ν_0, ν_1 are the reluctivities of the air and ferromagnetics, respectively. Finally, let $\mathcal{I} : \mathbf{L}^2(\Omega) \to \mathbf{R}$ be a cost functional, possibly involving penalization of state constraints. Given a maximal volume $V_{\max}$ of the designed structure, the 3D topology optimization problem governed by the linear magnetostatics then reads as follows:

$$\left\{\begin{array}{l} \qquad\qquad\qquad \min\limits_{\rho \in \mathcal{Q}} \mathcal{I}(\mathbf{curl}(\mathbf{u})) \\ \text{w.r.t.} \\ \qquad\qquad\qquad \int\limits_{\Omega_\mathrm{d}} \widetilde{\rho}(\rho)\, d\mathbf{x} \le V_{\max} \\ \int\limits_{\Omega} \nu\left(\widetilde{\rho}(\rho)\right) \mathbf{curl}(\mathbf{u}) \cdot \mathbf{curl}(\mathbf{v})\, d\mathbf{x} = \int\limits_{\Omega} \mathbf{J} \cdot \mathbf{v}\, d\mathbf{x} \text{ in } \mathbf{H}_{\mathbf{0},\perp}(\mathbf{curl}; \Omega), \end{array}\right. \tag{1}$$

where $\mathbf{J} \in \mathbf{L}^2(\Omega)$ is a divergence–free current density and where

$$\mathbf{H}_{\mathbf{0},\perp}(\mathbf{curl}; \Omega) := \{\mathbf{v} \in \mathbf{H}_\mathbf{0}(\mathbf{curl}; \Omega) \mid \forall p \in H^1_0(\Omega) : \int_\Omega \mathbf{grad}(p) \cdot \mathbf{v}\, d\mathbf{x} = 0\},$$

$$\mathbf{H}_\mathbf{0}(\mathbf{curl}; \Omega) := \{\mathbf{v} \in \mathbf{L}^2(\Omega) \mid \mathbf{curl}(\mathbf{v}) \in L^2(\Omega)\}.$$

Note that the 2-dimensional (2D) reduced magnetostatic problem leads to the Poisson equation.

Concerning the numerical solution, the 3-dimensional (3D) problem is discretized by the finite element method using the lowest order edge Nédélec elements on tetrahedra, while we use the lowest order nodal Langrange elements on triangles in case of the 2D reduced problem. The design material distribution is elementwise constant. Note that in the 3D case we do not solve the mixed formulation in $\mathbf{H}_{\mathbf{0},\perp}(\mathbf{curl};\Omega)$ but rather a non-mixed one in $\mathbf{H}_{\mathbf{0}}(\mathbf{curl};\Omega)$ while we add the regularization term $\varepsilon\int_\Omega \mathbf{u}\cdot\mathbf{v}\,d\mathbf{x}$ to the bilinear form. In the optimization process we always choose the initial value of ρ to be 0.5.

3 Piecewise Smooth Approximation of Shapes

We will use the optimal topology design as the initial guess for the shape optimization. The first step towards a fully automatic procedure is a shape identification, which we are doing by hand for the moment. The second step we are treating now is a piecewise smooth approximation of the shapes by Bézier curves or patches. Let $\rho^{\mathrm{opt}} \in \mathcal{Q}$ be an optimized discretized material distribution. Recall that it is not a strictly 0-1 function. Let $\mathbf{p}_1,\dots,\mathbf{p}_n$ denote vectors of Bézier parameters of the shapes $\alpha_1(\mathbf{p}_1),\dots,\alpha_n(\mathbf{p}_n)$ which form the air and ferromagnetic subdomains $\Omega_0(\alpha_1,\dots,\alpha_n)$ and $\Omega_1(\alpha_1,\dots,\alpha_n)$, respectively, i.e. $\Omega_1\subset\Omega_{\mathrm{d}}$, $\overline{\Omega}=\overline{\Omega_0}\cup\overline{\Omega_1}$ and $\Omega_0\cap\Omega_1=\emptyset$. Let further $\underline{\mathbf{p}_i}$ and $\overline{\mathbf{p}_i}$ denote the lower and upper bounds, respectively, and let $\mathcal{P} := \left\{(\mathbf{p}_1,\dots,\mathbf{p}_n)\mid \underline{\mathbf{p}_i}\le\mathbf{p}_i\le\overline{\mathbf{p}_i} \text{ for } i=1,\dots,n\right\}$ be the set of admissible Bézier parameters. We solve the following least square fitting problem:

$$\min_{(\mathbf{p}_1,\dots,\mathbf{p}_n)\in\mathcal{P}} \int_{\Omega_{\mathrm{d}}} \left(\rho^{\mathrm{opt}} - \chi(\Omega_1\left(\alpha_1(\mathbf{p}_1),\dots,\alpha_n(\mathbf{p}_n)\right))\right)^2\,d\mathbf{x}, \tag{2}$$

where $\chi(\Omega_1)$ is the characteristic function of Ω_1.

When solving (2) numerically, one encounters the problem of intersection of the Bézier shapes with the mesh on which ρ^{opt} is elementwise constant. In order to avoid it we use the property that the Bézier control polygon converges quite fast to the shape under the refinement procedure, which is in 2D as follows:

$$\begin{aligned}\left[\mathbf{p}_i^{k+1}\right]_0 &:= \left[\mathbf{p}_i^{k}\right]_0\\ \left[\mathbf{p}_i^{k+1}\right]_j &:= \tfrac{j-1}{m_i+1}\left[\mathbf{p}_i^{k}\right]_{j-1} + \tfrac{n-j}{m_i+1}\left[\mathbf{p}_i^{k}\right]_j,\ j=2,\dots,m_i\\ \left[\mathbf{p}_i^{k+1}\right]_{m_i+1} &:= \left[\mathbf{p}_i^{k}\right]_{m_i}\end{aligned} \tag{3}$$

where $\mathbf{p}_i^0 := \mathbf{p}_i$, see also Fig. 1. Note that in 3D one uses a similar procedure provided a tensor-product grid of Bézier control nodes. Then the integration in (2) is replaced by a sum over the elements and we deal with intersecting the mesh with a polygon. Note that our least square functional is not twice differentiable whenever a shape touches the grid. This is still acceptable for the quasi-Newton optimization method that we apply.

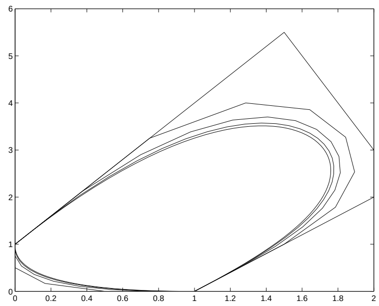

Fig. 1. Approximation of Bézier shapes by the refined control polygon

4 Multilevel Shape Optimization for Magnetostatics

With the notation of Sect. 2, the shape optimization problem under consideration is as follows:

$$\left\{\begin{array}{l} \displaystyle\min_{(\mathbf{p}_1,\dots,\mathbf{p}_n)\in\mathcal{P}} \mathcal{I}(\mathbf{curl}(\mathbf{u})) \\ \text{w.r.t.} \\ \displaystyle\int_{\Omega_1(\alpha_1(\mathbf{p}_1),\dots,\alpha_n(\mathbf{p}_n))} d\mathbf{x} \le V_{\max} \\ \displaystyle\sum_{i=0}^{1} \int_{\Omega_i(\alpha_1(\mathbf{p}_1),\dots,\alpha_n(\mathbf{p}_n))} \nu_i \mathbf{curl}(\mathbf{u})\cdot\mathbf{curl}(\mathbf{v})\, d\mathbf{x} = \int_{\Omega} \mathbf{J}\cdot\mathbf{v}\, d\mathbf{x} \text{ in } \mathbf{H}_{\mathbf{0},\perp}(\mathbf{curl};\Omega). \end{array}\right. \tag{4}$$

Again, we use the regularization and the 2D reduction as in Sect. 2

Concerning the discretization, we have to take special care of how the shape enters the bilinear form in order not to change the topology of the mesh. We use two approaches here. First, the control design nodes interpolate the Bézier shape and the remaining grid nodes displacements are given by solving an auxiliary discretized linear elasticity problem with the nonzero Dirichlet boundary condition along the design shape. The drawback is that on fine meshes some elements may flip whenever the shape changes significantly. Another approach is to use (3) again and intersect the refined Bézier control polygon with the mesh so that the design interface goes across some elements. This brings a little nonsmoothness, which is still acceptable for a quasi-Newton optimization method we use. Moreover, assembling the bilinear form takes much longer. On the other hand, the design change is not limited by the finesty of the grid.

Perhaps, the main reason for solving the coarse topology optimization as a preprocessing is that we get rid of a large number of design variables in cases of fine discretized topology optimization. Once we have a good initial shape design, we will proceed the shape optimization in a multilevel way in order to speed up the algorithm as much as possible. We propose to couple the outer quasi-Newton method with the nested conjugate gradient method preconditioned by a geometric multigrid (PCG), as depicted in Algorithm 1, in which $\mathbf{A}^l(\mathbf{p}_1, \ldots, \mathbf{p}_n)$ denotes the reluctivity matrix assembled at the l-th level.

Algorithm 1 Newton iterations coupled with nested multigrid PCG

Given $\mathbf{p}_1^{\text{init}}, \ldots, \mathbf{p}_n^{\text{init}}$
Discretize at the first level $\longrightarrow h^1, \mathbf{A}^1(\mathbf{p}_1^{\text{init}}, \ldots, \mathbf{p}_n^{\text{init}})$
Solve by a quasi-Newton method and the nested direct solver $\longrightarrow \mathbf{p}_1^1, \ldots, \mathbf{p}_n^1$
Store the first level preconditioner $\mathbf{C}^1 := \left[\mathbf{A}^1(\mathbf{p}_1^1, \ldots, \mathbf{p}_n^1)\right]^{-1}$
for $l = 2, \ldots$ **do**
  Refine $h^{l-1} \longrightarrow h^l$
  Prolong $\mathbf{p}_1^{l-1}, \ldots, \mathbf{p}_n^{l-1} \longrightarrow \mathbf{p}_1^{l,\text{init}}, \ldots, \mathbf{p}_n^{l,\text{init}}$
  Solve by a quasi-Newton method and the nested multigrid solver $\longrightarrow \mathbf{p}_1^l, \ldots, \mathbf{p}_n^l$
  Store the l–th level preconditioner $\mathbf{C}^l$
end for

5 An Application

We consider a direct electric current (DC) electromagnet, see Fig. 2. The

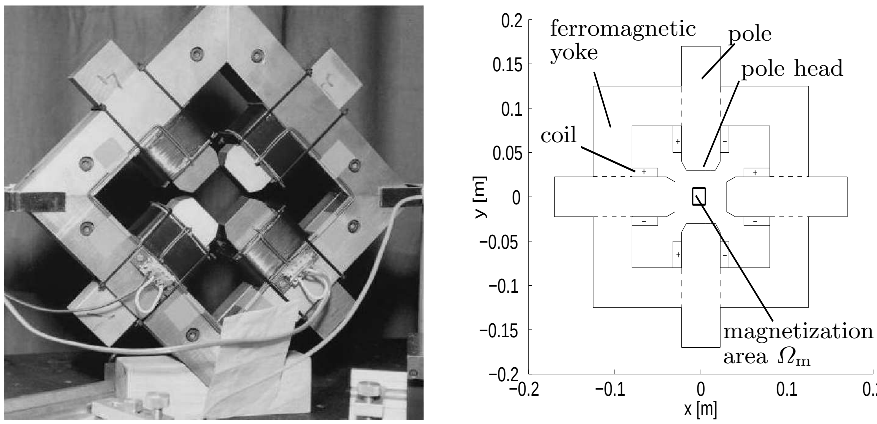

Fig. 2. An electromagnet of the Maltese Cross geometry

electromagnets are used for measurements of Kerr magnetooptic effects, cf. [ZK97]. They require the magnetic field among the pole heads as homogeneous, i.e. as constant as possible. Let us note that the magnetooptic effects are investigated for applications in high capacity data storage media, like development of new media materials for magnetic or compact discs recording. Let us also note that the electromagnets have been developed at the Institute of Physics, Technical University of Ostrava, Czech Republic, see [Pos02]. A number of instances have been delivered to laboratories in France, Canada or Japan.

Our aim is to improve the current geometries of the electromagnets in order to be better suited for measurements of the Kerr effect. The generated magnetic field should be strong and homogeneous enough. Unfortunately, these assumptions are contradictory and we have to balance them. The cost functional reads as follows:

$$\mathcal{I}(\mathbf{curl}(\mathbf{u})) := \int_{\Omega_\mathrm{m}} \|\mathbf{curl}(\mathbf{u}) - B_\mathrm{m}^\mathrm{avg}\mathbf{n}_\mathrm{m}\|^2 + 10^6 \left(\min\{0, B_\mathrm{m}^\mathrm{avg} - B^\mathrm{min}\}\right)^2,$$

where $\Omega_\mathrm{m} \subset \Omega$ is the subdomain where the magnetic field should be homogeneous, $B_\mathrm{m}^\mathrm{avg}$ is the mean value over Ω_m of the magnetic flux density component in the direction $\mathbf{n}_\mathrm{m} := (0,1)$ and $B^\mathrm{min} := 0.12\,[\mathrm{T}]$ is the minimal required magnitude. There are 600 turns pumped by the current of $5\,[\mathrm{A}]$. We use the linearized value of the relative permeability of the ferromagnetics, which is 5100. Some results were already presented in [Luk01].

6 Numerical Results

We present numerical results for our application in 2D. For simplicity we consider only two coils to be active and take, due to the symmetry, a quarter of the domain, see Fig. 3 **(a)**. Given the initial design $\rho^\mathrm{init} := 0.5$ in Ω_d we start with the topology optimization. Concerning (1), we choose $V_\mathrm{max} := 0.0155\,[\mathrm{m}^2]$ and $p := 100$. A coarse optimized topology design is depicted in Fig. 3 **(b)**. There are 861 design, 1105 state variables and the optimization was done in 7 steepest descent iterations which took 2.5 seconds, when using the adjoint method for the sensitivity analysis.

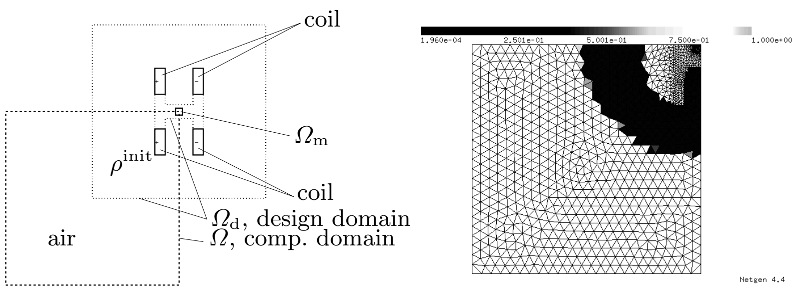

Fig. 3. Topology optimization: **(a)** initial design; **(b)** coarsely optimized design ρ^opt

The second part of the computation is the shape approximation. Here we refer to Fig. 4. We are looking for three Bézier curves that fit the optimized topology. Here we have 19 design parameters in total and solving the least square problem (2) was finished in 8 quasi-Newton iterations which took 26 seconds, when using the numerical differentiation.

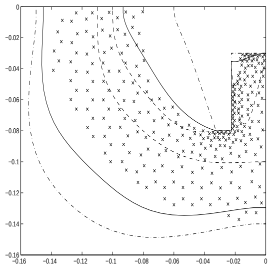

Fig. 4. Shape approximation: dashed line – lower bound; dash-and-dot line – upper bound; solid line – optimal shape approximation; crosses – mid-points of the elements with $\rho^{\mathrm{opt}} \geq 0.5$

Finally, we used the smooth shape design as the initial guess for the shape optimization (4). In Tables 1 and 2 there are parameters of the computation when using the mesh deformation and the so-called shape-across-elements approach, respectively. In the first case the multigrid acts very efficiently, however, on the finest level we end up with the design almost the same as the very initial one $\mathbf{p}_1^{1,\mathrm{init}}, \ldots, \mathbf{p}_n^{1,\mathrm{init}}$. This is due to that the mesh deformation is very limited at the finest mesh. In the second approach we observed a significant improvement of the shape in terms of the cost functional, however, the multigrid preconditioner is by far not efficient, see Table 2, due to the reluctivity being jumping within some elements. The final optimized geometry calculated by the second approach is depicted in Fig. 5 **(a)**. We can see that the result is in a good correspondance with the so-called O-Ring electromagnet which was already designed and manufactured by physicists.

Table 1. Multilevel shape optimization using the mesh deformation approach

level	design variables	outer Newton iterations	state variables	nested CG iterations	total time
1	19	7	1098		27s
2	40	8	4240	3	3min 9s
3	82	8	16659	4–5	29min 14s
4	166	8	66037	4–5	3h 37min 42s

Table 2. Multilevel shape optimization using the shape-across-elements approach

level	design variables	outer Newton iterations	state variables	nested CG iterations	total time
1	19	14	1098		4min 32s
2	40	6	4240	11–14	26min 37s
3	82	8	16659	21–26	3h 20min 15s

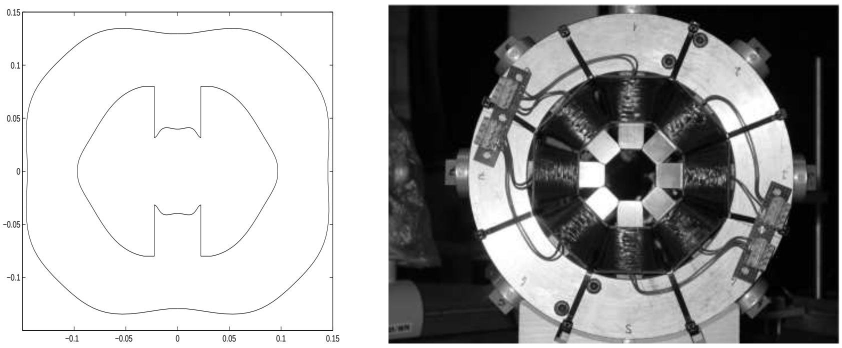

Fig. 5. Multilevel shape optimization: **(a)** optimized geometry; **(b)** the O-Ring electromagnet

7 Conclusion

This paper presented a method which sequentially combines topology and shape optimization. First, we solved a coarsely discretized topology optimization problem. Then we approximated some chosen interfaces by Bézier shapes. Finally, we proceeded with shape optimization in a multilevel way. We also discussed two different shape-to-state mappings. We applied the method to a 2D optimal shape design of a DC electromagnet. Without the multilevel procedure, we can get already fine optimized geometries in minutes. However, as we aim at large-scale discretizations, it still remains to analyze and improve the multigrid convergence.

References

[Ben95] Bendsøe, M.P.: Optimization of Structural Topology, Shape and Material. Springer, Berlin, Heidelberg (1995)

[Cea00] Céa, J., Garreau, S., Guillaume, P., Masmoudi, M.: The shape and topological optimizations connection. Comput. Methods Appl. Mech. Eng. **188**, 713–726 (2000)

[HN97] Haslinger J., Neittaanmäki P.: Finite Element Approximation for Optimal Shape, Material and Topology Design. Wiley, Chinchester (1997)

[Luk01] Lukáš, D.: Shape optimization of homogeneous electromagnets. In: van Rienen, U., Günther, M., Hecht, D. (eds.) Scientific Computing in Electrical Engineering 2000, Lect. Notes Comp. Sci. Engrg. **18**, pp. 145–152 (2001)

[Luk04] Lukáš, D.: On solution to an optimal shape design problem in 3-dimensional magnetostatics. Appl. Math. **49**:5, 24 pp. (2004)

[OBR91] Olhoff, N., Bendsøe, M.P., Rasmussen, J.: On CAD-integrated structural topology and design optimization. Comp. Meth. Appl. Mech. Eng. **89**, 259–279 (1991)

[Pos02] Postava, K., Hrabovský, D., Pištora, J., Fert, A.R., Višňovský, Š., Yamaguchi, T.: Anisotropy of quadratic magneto-optic effects in reflection. J. Appl. Phys. **91**, 7293–7295 (2002)

[TCh01] Tang, P.-S., Chang, K.-H.: Integration of topology and shape optimization for design of structural components. Struct. Multidisc. Optim. **22**, 65–82 (2001)

[ZK97] Zvedin, A.K., Kotov, V.A.: Modern Magnetooptics and Magnetooptical Materials. Institute of Physics Publishing Bristol and Philadelphia (1997)